AFRL-ML-TY-TR-2004-4527

Simultaneous Measurement of Specific Discharge and Cr(VI) Mass Flux in Porous Media Using Permeable Adsorbent Device

Timothy J. Campbell, Kirk Hatfield*, and Michael D. Annable
Department of Civil Engineering, University of Florida
345 Weil Hall
Gainesville, Florida 32603

P.S.C. Rao
School of Civil Engineering, Purdue University
1284 Civil Engineering Building
West Lafayette, IN 47907

AIR FORCE RESEARCH LABORATORY
MATERIALS & MANUFACTURING DIRECTORATE
AIRBASE TECHNOLOGIES DIVISION
139 BARNES DRIVE, STE 2
TYNDALL AFB FL 32403-5323

NOTICES

USING GOVERNMENT DRAWINGS, SPECIFICATIONS, OR OTHER DATA INCLUDED IN THIS DOCUMENT FOR ANY PURPOSE OTHER THAN GOVERNMENT PROCUREMENT DOES NOT IN ANY WAY OBLIGATE THE US GOVERNMENT. THE FACT THAT THE GOVERNMENT FORMULATED OR SUPPLIED THE DRAWINGS, SPECIFICATIONS, OR OTHER DATA DOES NOT LICENSE THE HOLDER OR ANY OTHER PERSON OR CORPORATION; OR CONVEY ANY RIGHTS OR PERMISSION TO MANUFACTURE, USE, OR SELL ANY PATENTED INVENTION THAT MAY RELATE TO THEM.

THIS REPORT IS RELEASABLE TO THE NATIONAL TECHNICAL INFORMATION SERVICE
5285 PORT ROYAL RD.
SPRINGFIELD VA 22 161
TELEPHONE 703 487 4650; 703 4874639 (TDD for the hearing-impaired)
E-MAIL orders@ntis.fedworld.gov
WWW http://www.ntis.gov/index.html

AT NTIS, IT WILL BE AVAILABLE TO THE GENERAL PUBLIC, INCLUDING FOREIGN NATIONS.

THIS TECHNICAL REPORT HAS BEEN REVIEWED AND IS APPROVED FOR PUBLICATION.

//s//
KOLIN C. NEWSOME, 2d Lt, USAF
Program Manager

//s//
MICHAEL J. CALIDONNA, Major, USAF
Chief, Weapons Systems Logistics Branch

//s//
JIMMY L. POLLARD, Colonel, USAF
Chief, Airbase Technologies Division

Do not return copies of this report unless contractual obligations or notice on a specific document requires its return.

REPORT DOCUMENTATION PAGE

Form Approved
OMB No. 0704-0188

1. AGENCY USE ONLY *(Leave blank)*	2. REPORT DATE	3. REPORT TYPE AND DATES COVERED
	August 2001	Final Report

4. TITLE AND SUBTITLE
Simultaneous Measurement of Specific Discharge and Cr(VI) Mass Flux in Porous Media Using Permeable Adsorben Device

5. FUNDING NUMBERS
JON: RUFLB78A

6. AUTHORS
Timothy J. Campbell, Kirk Hatfield, Michael D. Annable

7. PERFORMING ORGANIZATION NAME(S) AND ADDRESS(ES)
Department of Civil Engineering, University of Florida
345 Weil Hall
Gainsville, FL 32603

8. PERFORMING ORGANIZATION REPORT NUMBER
AFRL ML-TY-TR-2004-4527

9. SPONSORING/MONITORING AGENCY NAME(S) AND ADDRESS(ES)
Air Force Research Laboratory (MLQL)
139 Barnes Drive, Suite 2
Tyndall AFB FL 32403

10. SPONSORING/MONITORING AGENCY REPORT NUMBER
N/A

11. SUPPLEMENTARY NOTES

12a. DISTRIBUTION/AVAILABILITY STATEMENT
Distribution Unlimited; Approved for Public Release

12b. DISTRIBUTION CODE
A

13. ABSTRACT *(Maximum 200 words)* The method for simultaneous measurement of local groundwater specific discharge (**q**) and Cr(VI) mass flux ($\mathbf{J}^{Cr}$) using a permeable adsorbent device is proposed. The proposed method allows for determination of both **q** and $\mathbf{J}^{Cr}$ as two-dimensional vectors, with each vector composed of an angular (q_θ, J_θ^{Cr}) and a radial (q_r, J_r^{Cr}) component. The device consists of a cylindrical container whose outer shell is constructed of highly permeable mesh material with impermeable end caps. The interior of the device is divided into a center well and three outer sectors, each packed with a granular anion exchange resin having high adsorption capacity for the Cr(VI) oxyanions CrO_4^{2-} and $HCrO_4^-$. The adsorbent in the center well of the device is loaded with benzoate as resident tracer. Experiments were conducted in which these devices were placed in porous packed bed columns through which was passed a measured quantity of simulated groundwater containing Cr(VI). The resin was then removed from the four sectors separately and extracted to determine the masses of Cr(VI) and resident tracer bound in each. A linear solute transport model was used to relate the observed rate of resident tracer displacement to q_θ and q_r, and a simple mass balance equation was used to calculate J_r^{Cr}. Experimental results showed q_θ was measured to an accuracy of $\pm 15^\circ$. Accuracy of the radial specific discharge vector component depended on the degree of displacement of the resident tracer. J_r^{Cr} mass flux vector radial component was measured to an accuracy of $\pm$ 17%. These results demonstrate that the proposed method represents a promising technique for determination of specific discharge and contaminant mass flux in contaminated aquifers.

14. SUBJECT TERMS
Chromium(VI), adsorbent, groundwater, microbial degradation

15. NUMBER OF PAGES
28

16. PRICE CODE

17. SECURITY CLASSIFICATION OF REPORT	18. SECURITY CLASSIFICATION OF THIS PAGE	19. SECURITY CLASSIFICATION OF ABSTRACT	20. LIMITATION OF ABSTRACT
UNCLASSIFIED	UNCLASSIFIED	UNCLASSIFIED	UL

Simultaneous Measurement of Specific Discharge and Cr(VI) Mass Flux in Porous Media Using Permeable Adsorbent Device

Timothy J. Campbell, Kirk Hatfield*, and Michael D. Annable

Department of Civil Engineering, University of Florida

345 Weil Hall

Gainesville, Florida 32603

P.S.C. Rao

School of Civil Engineering, Purdue University

1284 Civil Engineering Building

West Lafayette, IN 47907

*Corresponding author phone: (352) 392-9537 ext 1441, fax: (352) 392-3394,

e-mail: khatf@ce.ufl.edu

Abstract

In this paper a method is proposed for simultaneous measurement of local groundwater specific discharge (**q**) and Cr(VI) mass flux ($\mathbf{J}^{Cr}$) using a permeable adsorbent device. The proposed method allows for determination of both **q** and $\mathbf{J}^{Cr}$ as two-dimensional vectors, with each vector composed of an angular (q_θ, J_θ^{Cr}) and a radial (q_r, J_r^{Cr}) component. The device consists of a cylindrical container whose outer shell is constructed of highly permeable mesh material with impermeable end caps. The interior of the device is divided into a center well and three outer sectors, each packed with a granular anion exchange resin having high adsorption capacity for the Cr(VI) oxyanions CrO_4^{2-} and $HCrO_4^-$. The adsorbent in the center well of the device is loaded with benzoate as resident tracer. Experiments were conducted in which these devices were placed in porous packed bed columns through which was passed a measured quantity of simulated groundwater containing Cr(VI). The resin was then removed from the four sectors separately and extracted to determine the masses of Cr(VI) and resident tracer bound in each. A linear solute transport model was used to relate the observed rate of resident tracer displacement to q_θ and q_r, and a simple mass balance equation was used to calculate J_r^{Cr}. Experimental results showed q_θ was measured to an accuracy of $\pm$ 15°. Accuracy of the radial specific discharge vector component depended on the degree of displacement of the resident tracer. J_r^{Cr} mass flux vector radial component was measured to an accuracy of $\pm$ 17%. These results demonstrate that the proposed method represents

a promising technique for determination of specific discharge and contaminant mass flux in contaminated aquifers.

Introduction

Chromium is one of the most common and persistent groundwater pollutants in the United States (*1*). A considerable amount of laboratory research has been devoted to the study of processes that effect the concentration and speciation of chromium in aqueous systems. These processes include reduction of hexavalent chromium (Cr(VI)), the most toxic and mobile oxidation state of chromium, to the less mobile and less toxic Cr(III) by abiotic (*2, 3*) and microbially-mediated (*4, 5, 6*) redox processes, adsorption of Cr(VI) oxyanions on metal oxides (*7, 8, 9*), microbial biosorption of Cr(VI) (*10*), oxidation of Cr(III) to Cr(VI) by dissolved oxygen (*11*), photoreduction of Cr(VI) (*12*), and precipitation of Cr(III) hydroxides (*13*).

Chromium transport in polluted groundwater has also been studied extensively (*14, 15, 16*). However, interpretation of the results of these field studies is confounded by the complexity of Cr(VI) chemistry in natural systems (*17*). In addition to the above processes, Cr(VI) concentration in groundwater can be influenced by dilution due to aquifer recharge downstream from a source zone. Since volumetric recharge rates usually can only be estimated approximately, the effect of aquifer recharge on Cr(VI) concentration cannot be known with a high degree of certainty. This uncertainty prohibits accurate determination of Cr(VI) attenuation rates at affected sites. In principle,

attenuation rates can be measured more accurately using contaminant mass flux rather than concentration. The mass flux $\mathbf{J}^i$ of a contaminant i is the product of concentration C^i and specific discharge $\mathbf{q}$, i.e. $\mathbf{J}^i = C^i\mathbf{q}$. (Note that in this paper, 2-dimensional vectors are indicated by boldface, while scalar quantities are in regular typeface.) Since recharge flow to an aquifer element increases $\mathbf{q}$ and decreases C^i by the same factor, $\mathbf{J}^i$ is independent of recharge rate. Monitoring Cr(VI) attenuation rates through measurement of Cr(VI) mass flux $\mathbf{J}^{Cr}$ in addition to or instead of concentration C^{Cr} could therefore lead to greater accuracy by eliminating the uncertainty in estimated recharge rates. The ability to directly measure $\mathbf{J}^{Cr}$ could also be of significant use in predicting the impact of a Cr(VI) source zone on a down-gradient drinking water supply well. The impact of a contaminant source on a downstream supply well can be predicted using a mass balance estimation (*18*), but this approach relies on a number of conditions which often are not satisfied. Direct measurement of $\mathbf{J}^{Cr}$ and $\mathbf{q}$ across a transect of a Cr(VI) plume over a long sampling period would permit more accurate estimation of future C^{Cr} levels in the supply well, by minimizing or eliminating reliance on assumptions of constant flow field and constant source zone release rate.

In this paper, we propose a general method for simultaneous measurement of groundwater $\mathbf{q}$ and $\mathbf{J}^i$ in contaminated aquifers using a permeable adsorbent device. In concept, the device consists of a permeable cylindrical shell packed with a porous bed of adsorbent material having a high sorption capacity for the groundwater contaminant of interest. The ends of the cylinder are capped with impermeable material. The interior of

the device is divided by permeable walls into four sectors, a center well and three equal-volume outer sectors, as shown in Figure 1. A quantity of a reversibly-adsorbed resident tracer compound is uniformly distributed on the adsorbent in the center well, while the adsorbent in the three outer sectors contains no resident tracer. Sampling is initiated at some time t = 0 (Fig. 1a) when the device is inserted into a sampling well in the contaminated aquifer. Horizontal infiltration of groundwater through the device due to local hydraulic gradients causes accumulation of sorbed contaminant in the upgradient sectors of the device, while the passage of groundwater through the center well displaces resident tracer into the downgradient sectors. After a sampling period Δt (Fig. 1b) the device is removed from the sampling well. The adsorbent material is removed separately from each of the outer sectors of the device, extracted, and the extract fractions analyzed to determine the masses of resident tracer and contaminant adsorbed in each sector at Δt. Groundwater $\mathbf{q}$ and $\mathbf{J}^i$ can then be calculated as two-dimensional vectors using relationships derived from simple solute transport models.

The general method described above could be applied to measurement of $\mathbf{J}^{Cr}$ if the appropriate adsorbent and resident tracer were selected. Since Cr(VI) in dilute aqueous solutions at near-neutral pH is present predominately as the oxyanions chromate (CrO_4^{2-}) and bichromate ($HCrO_4^-$), and at higher concentrations as dichromate ($Cr_2O_7^{2-}$) (*19*), an anion exchange resin would seem to be an appropriate choice of adsorbent, and any stable anionic compound with the appropriate partitioning behavior could be used as the resident tracer. The objective of the present study was to evaluate, using laboratory

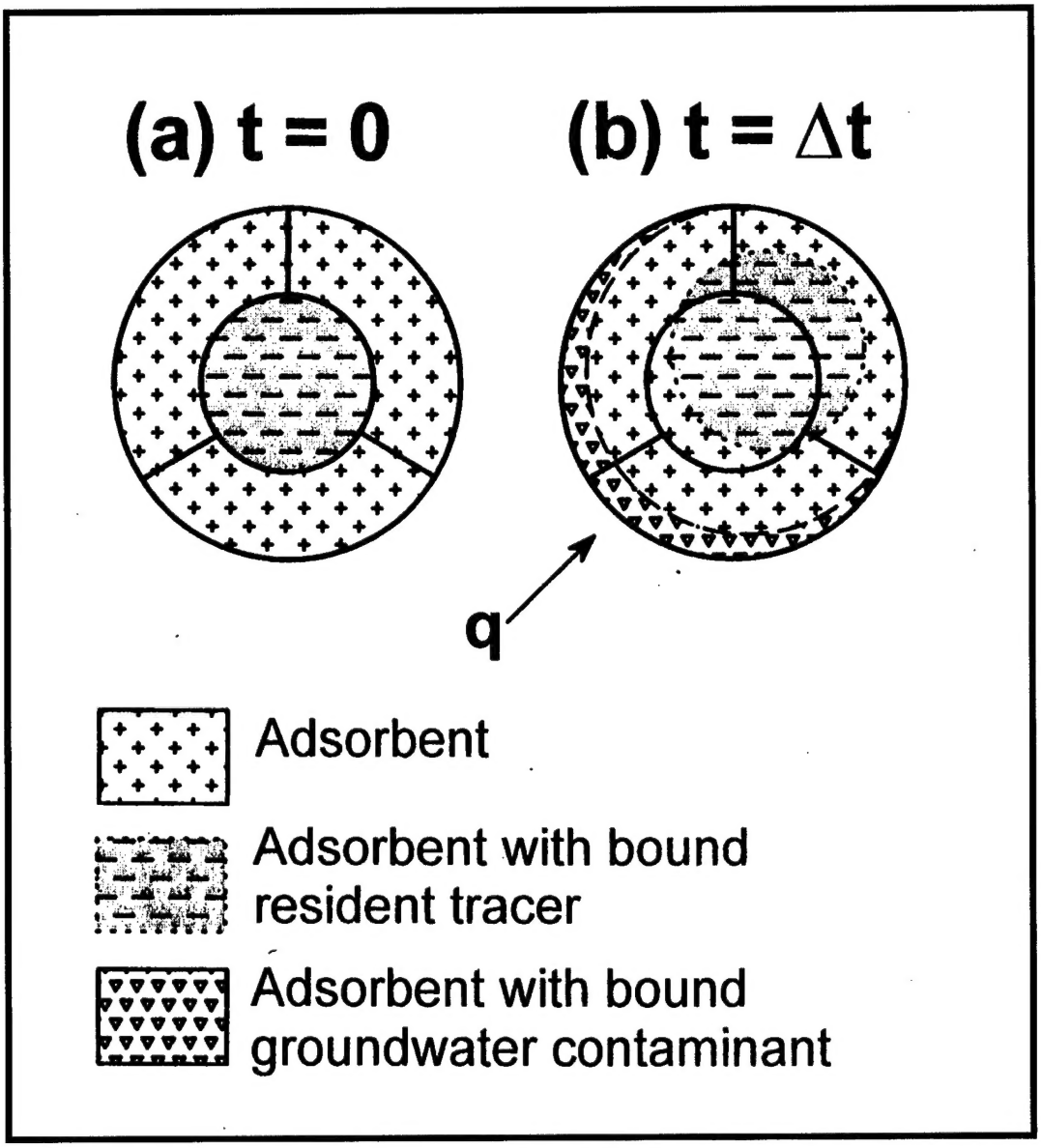

Figure 1. Conceptual diagram showing operation of a permeable adsorbent device for simultaneous measurement of groundwater specific discharge and contaminant mass flux. (a) Device as entered in porous media. (b) Device after a sampling period Dt.

experiments, the usefulness of permeable packed bed devices containing anion exchange adsorbent for simultaneous measurement of **q** and $\mathbf{J}^{Cr}$ in porous media. Experiments were designed to assess the accuracy of the devices in conditions that simulate contaminated groundwater flow in an idealized aquifer system. Experimental parameters were selected to reveal the limits of the device's useful range in the measurement of the vectors **q** and $\mathbf{J}^{Cr}$.

Experimental Section

Chemicals. Benzoic acid (J.T. Baker, Phillipsburg, N.J.) stock solution was prepared by dissolving 1.00 g of the free acid in 10.0 mL HPLC grade methanol (Fisher Scientific, Fair Lawn, NJ). A 2.0 g L^{-1} Cr(VI) stock solution was prepared by dissolving 565 mg potassium dichromate (J.T. Baker) in 100 mL deionized water. Salt stock solution was prepared by dissolving the following in 1.0 L deionized water: 15 g sodium phosphate monobase hydrate (Fisher), 2.5 g each calcium chloride dihydrate (Aldrich), potassium chloride (Sigma, St. Louis, MO), sodium chloride (Aldrich), magnesium chloride hexahydrate (Fisher), magnesium sulfate heptahydrate (Sigma), 125 mg manganese chloride tetrahydrate (Aldrich), and 25 mg sodium molybdate dihydrate (Fisher). Simulated groundwater buffer (SGB) was made by dissolving 5.00 g sodium bicarbonate (Aldrich) in about 8 L deionized water, then adding 100 mL salts stock and diluting to 10.0 L. SGB had pH 7.0 ± 0.1, ionic strength 9.1 mM, and conductivity 0.8 mS. Resin

extraction solution was 1M sodium chloride in deionized water with pH adjusted to 11 using 2N NaOH. Deionized water used was >18 MΩ. AG1-X8 anion exchange resin, 20-50 mesh, 1.2 meq ml^{-1} capacity, was obtained in the hydroxide form from Bio-Rad Laboratories (Hercules, CA), and was converted to the bicarbonate form by washing slowly with 12 bed volumes 1M $NaHCO_3$, then 12 bed volumes of deionized water. The wet, drained AG1-X8(HCO_3^-) resin had bed density (ρ^{Resin}) 0.75 g cm^{-3}, and the resin bed porosity (ε^{Resin}) was measured to be 0.50. Benzoate resident tracer compounds were loaded onto the resin after the OH^- to HCO_3^- conversion by stirring 10 mL of resin in 50 mL deionized water, then adding 50 μL 2N NaOH and 200 μL benzoic acid stock solution. After 1 hour of stirring the loaded resin was dump-packed into a glass column and washed with 20 bed volumes of deionized water. Initial adsorbed concentration of benzoate on the resin was neither measured nor carefully controlled; however, the maximum adsorbed benzoate concentration obtainable by this procedure (assuming all added benzoate adsorbed) was 2 mg mL^{-1}, or 0.016 meq mL^{-1}, less than 2% of total resin capacity. Resin portions with and without loaded tracers were stored slurried in deionized water at room temperature before use.

Cr(VI), Benzoate Isotherms. Adsorption isotherm data points on AG1-X8(HCO_3^-) resin were acquired using 10 cm^3 glass vials. To each tared vial was added a portion of wet, drained resin weighed to the nearest mg, and 5.0 mL of SGB containing 2.0 mg mL^{-1} of either Cr(VI) or sodium benzoate. Duplicate control vials contained no resin. All vials were sealed with teflon-lined septa, placed on a rotary shaker at 30 rpm and agitated for

>40h in a 20°C incubator. Aqueous phase concentrations (C_{Aq}, mg mL^{-1}) were determined as described below. Adsorbed masses were calculated from the difference in aqueous mass of solute between vials with and without resin. Adsorbed concentrations (C_{Sorb}, mg g^{-1}) were calculated based on the mass of wet, drained resin. Benzoate linear partitioning coefficient (k_D^B, mL g^{-1}) was calculated from the slope of the benzoate adsorption isotherm.

Media Permeability. The hydraulic conductivities of packed beds of AG1-X8 (HCO_3^-) resin and 1-mm glass beads (K^{Resin} and K^{Beads} respectively, cm s^{-1}) were measured using a simple constant head permeameter tube with cross-sectional area A_{bed} = 2.41 cm^2 and length L_{bed} = 10 cm. Steady flow Q (cm^3 s^{-1}) of SGB was measured at three different constant head differences Δh (cm) using a graduated cylinder and stopwatch, then hydraulic conductivity calculated as $K = QL_{bed}/(A_{bed}\Delta h)$ (*20*). For both media the three K measurements had relative standard deviations of < 1 %. The mean of the three measurements was taken as the hydraulic conductivity of the media.

Device Construction. Permeable adsorbent devices were constructed of 50 × 50 mesh milling grade woven wire cloth (McMaster-Carr Supply Company, Atlanta, GA) according to the design shown in Figure 2. The wire cloth material used was woven from 7.5 mil (0.19 mm) diameter 304 stainless steel wires, had nominal opening width of 0.318 mm, and was 39% open area. The outer shell of the device was formed by overlapping the ends of an 80 × 2.6 cm strip of wire cloth. The overlapping ends were

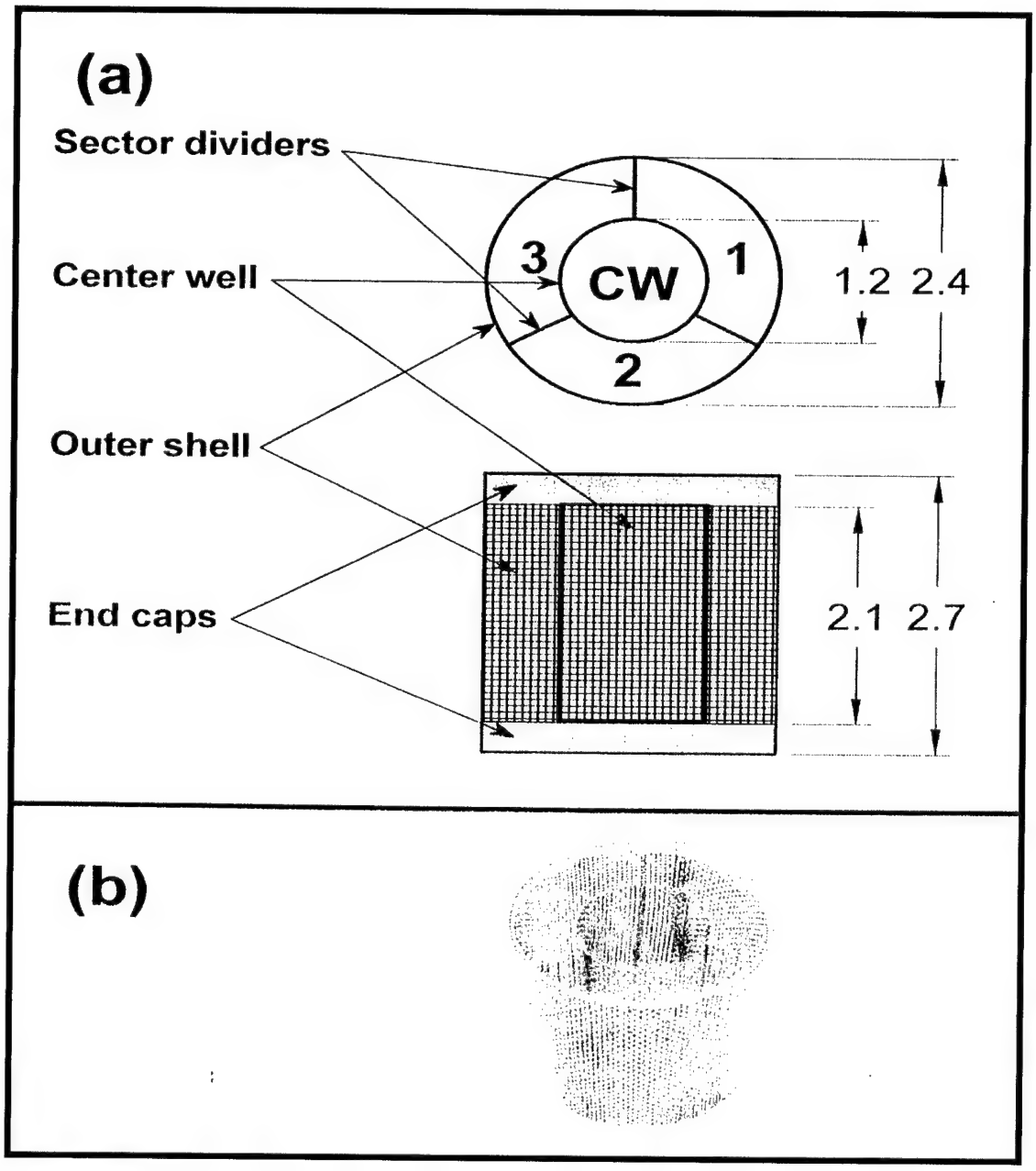

Figure 2. (a) Design and dimensions (cm) of permeable adsorbent devices used in this study. (b) Photograph of an empty device.

stitched together using wire unraveled from the cloth itself, forming a cylinder 2.4 cm in diameter. The center well was made the same way using a 4.0 × 2.1 cm strip of wire cloth to form a cylinder 1.2 cm in diameter. The outer sector dividers were 2.1 × 0.6 cm strips of wire cloth. These were joined to the center well at 120 degree spacings by pulling a wire out of the weave along one of the long ends of each strip, then inserting the protruding wires along that edge into the openings in the center well mesh. End caps were cut from 0.3 cm - thick cast acrylic clear sheet (McMaster-Carr) using a 1-inch diameter hole saw with no pilot bit. End caps cut this way fit tightly into the device outer shell and were held in place by friction. Devices constructed this way had outer diameter (D^{Dev}) 2.4 cm, center well diameter (D^{CW}) 1.2 cm, and bed length (L^{Dev}) 2.1 cm. Resin was packed into the devices as follows: an end cap was pressed into the outer shell first, then the center well with attached sector dividers was inserted into the shell. The sector dividers were arranged into a radial pattern, then the outer sectors were packed with AG1-X8 (HCO_3^-) resin. Once the outer sectors were packed, the resin served to hold the sector dividers firmly in place. Resin loaded with benzoate resident tracer was then packed into the center well, and the other end cap was pressed into place.

Column Experiments. Permeable adsorbent devices were tested in column systems configured as shown in Figure 3. The PVC columns had inner diameter (D^{Col}) 11.5 cm and length (L^{Col}) 6.5 cm. The column cross-sectional area (A^{Col}) was 104 cm^2. Columns were dump-packed with 4-mm glass beads (Fisher) to a depth of about 2 cm, then filled to the top with 1-mm glass beads (Supelco). A circle of woven wire cloth was used to

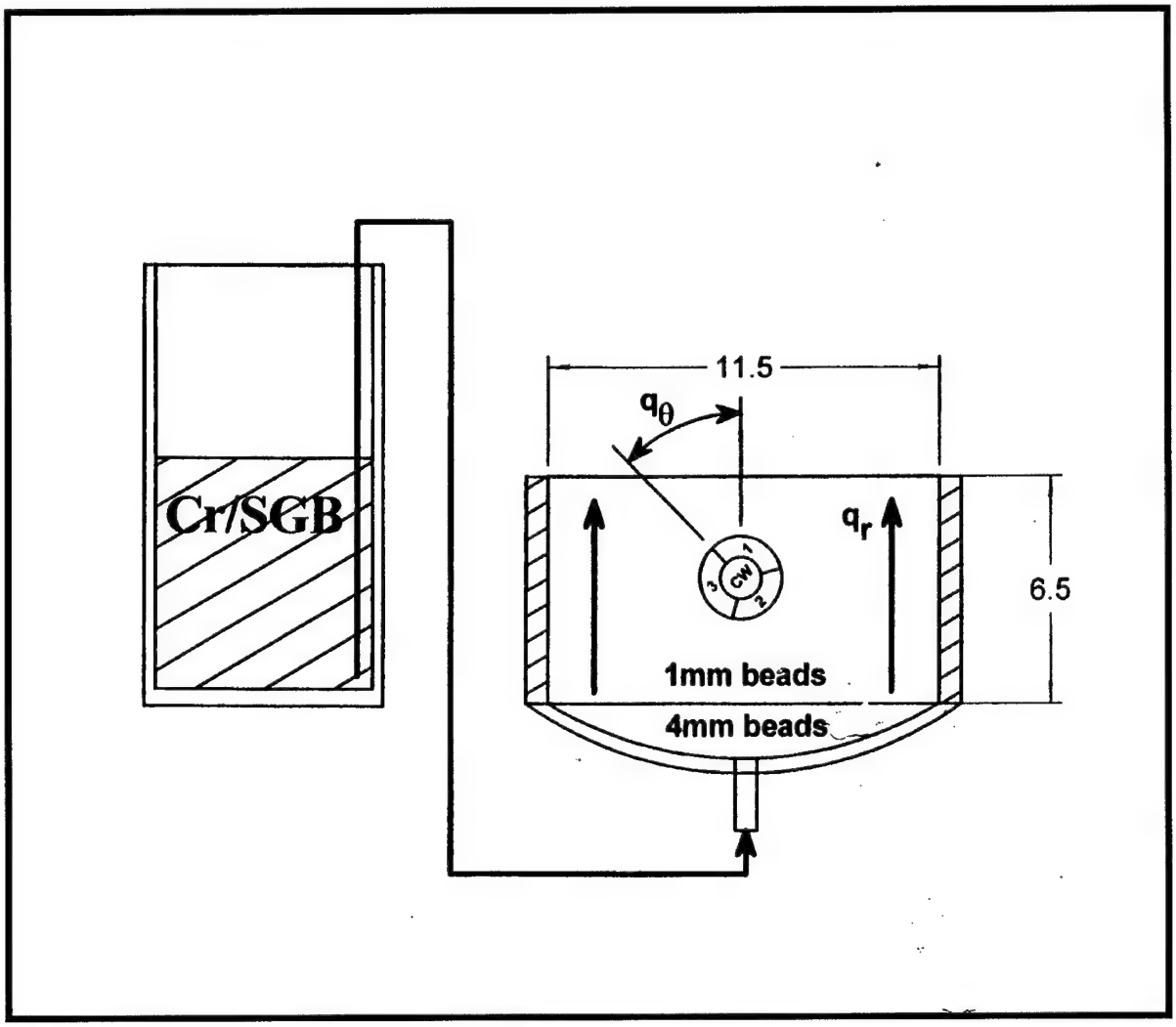

Figure 3. Schematic of porous media column systems used to conduct experiments with the permeable adsorbent devices. Column dimensions are given in cm.

separate the two bead layers. This design ensured that buffer fed through the bottom of the column was distributed at even pressure throughout the bottom section of the column, creating an even upward vertical flow profile throughout the 1-mm bead bed. After packing, columns were flushed with SGB containing 5 mg L^{-1} Cr(VI) (Cr/SGB). Flow through each column was siphoned via PVC tubing from a reservoir which was maintained at constant level by forced feed pumped from a main reservoir. Volumetric feed rates to the constant-level reservoirs were not precisely controlled and ranged from 3 to 10 mL min^{-1}. At t = 0 a permeable adsorbent device prepared as described above was buried in the glass bead bed to a depth of approximately 3 cm from the top edge of the device to the surface of the bed. The device was placed in the column with axis horizontal, and with the reference divider between outer sectors 1 and 3 rotated an angle q_θ from the vertical. Cr/SGB was then allowed to flow upward through the column, draining from the top of the bed through weir holes cut into the column rim. The Cr/SGB was collected as it drained from the column, and the collected volume was measured in a graduated cylinder to the nearest 0.1 L. After a volume ΔV (L) had been collected over a sampling period Δt (h), flow through the column was stopped and the device removed from the column. The Cr/SGB used in each run was analyzed separately to determine feed Cr(VI) concentration (C_F^{Cr}, mg L^{-1}). A total of 16 runs were conducted in a 4^2 experimental matrix, with the parameters q_θ and ΔV varied over 4 levels each. Experimental values of q_θ were 0, 45, 90, and 180 degrees, while ΔV levels were 4 –6 L, 8 –12 L, 19 – 21 L, and 30 – 42 L.

Analytical Methods. After removing the device from the column, one end cap was removed from the device, and the resin was scraped out of each sector individually, starting with the center well, using a round-end spatula. Care was taken to remove as much resin as possible from each sector without cross-contaminating resin in adjacent sectors. The resin from each sector was transferred to a 50-mL beaker, slurried in deionized water, then packed into a 1 cm ID glass column, and extracted with 20 mL resin extraction solution at 0.6 mL min^{-1}. This extraction technique was found to give Cr(VI) and benzoate recoveries of 100 ± 5% (data not shown). Extract fractions were assayed for Cr(VI) mass (m_i^{Cr}, mg) using the diphenylcarbazide colorimetric method (*21*). Response to Cr(VI) at 540 nm was calibrated using a 3-level standard curve. Benzoate resident tracer mass (m_i^{B}, mg) in the extract fractions was determined by HPLC using a 25.0 × 0.46 cm Partisil PAC 10μm column (Alltech Associates, Inc., Deerfield, IL). Mobile phase was 10% (v/v) HPLC-grade acetonitrile (Fisher), 90% 50 mM sodium phosphate pH 3.2, at 1.25 mL min^{-1}. The retention time of benzoic acid by this method was 4.3 min. Samples were diluted a minimum of 1:20 in mobile phase, then 0.25 mL was injected. Detection was by UV at 220 nm. Benzoate UV response factor was determined using a 3-level external standard calibration curve. A blank and a calibration check standard were analyzed with each set of samples to verify stable response.

Results and Discussion

Cr(VI) and benzoate adsorption isotherms at pH 7, 20°C are shown in Figure 4. Cr(VI) partitioning is nonlinear, as is expected for exchange of a divalent anion such as CrO_4^{2-} with a monovalent anion such as HCO_3^- (*22*). Benzoate partitioning is linear ($r^2 = 0.95$), with C^B_{Sorb} related to C^B_{Aq} by a linear partitioning coefficient (k_D^B, ml g^{-1})

$$C^B_{Sorb} = k^B_D C^B_{Aq} \quad [1]$$

The solid line in Figure 4 represents [1] with $k_D^B = 158$ mL g^{-1} for benzoate partitioning in SGB. Benzoate equilibrium partitioning on an anion exchange resin is influenced by the concentrations of competing anions in the aqueous phase. Since column experiments were conducted with buffer reservoirs open to the atmosphere, bicarbonate concentrations could have increased or decreased over time with CO_2 absorption or release. Therefore, it was important to verify that this k_D^B value was valid for each of the 16 column experiments. To verify this, the electrical conductivity of the Cr/SGB feed buffer was monitored for each column experiment, and was found to vary by < 8% over all runs. Using this k_D^B value with the AG1-X8 bed properties ρ^{Resin} and ε^{Resin}, a benzoate retardation coefficient (R^B) was calculated as

$$R^B = 1 + \frac{k^B_D \rho^{\text{Re sin}}}{\varepsilon^{\text{Re sin}}} = 238 \quad [2]$$

Hydraulic conductivities K^{Resin} and K^{Beads} were measured to be 0.39 and 0.84 cm s^{-1}, respectively. A hydraulic correction coefficient (K^{Corr}) was calculated as $K^{Corr} = (K^{Resin} +$

$K^{Beads})/2K^{Resin} = 1.57$ (*20*) to account for the difference between specific discharge inside the device and in the surrounding media.

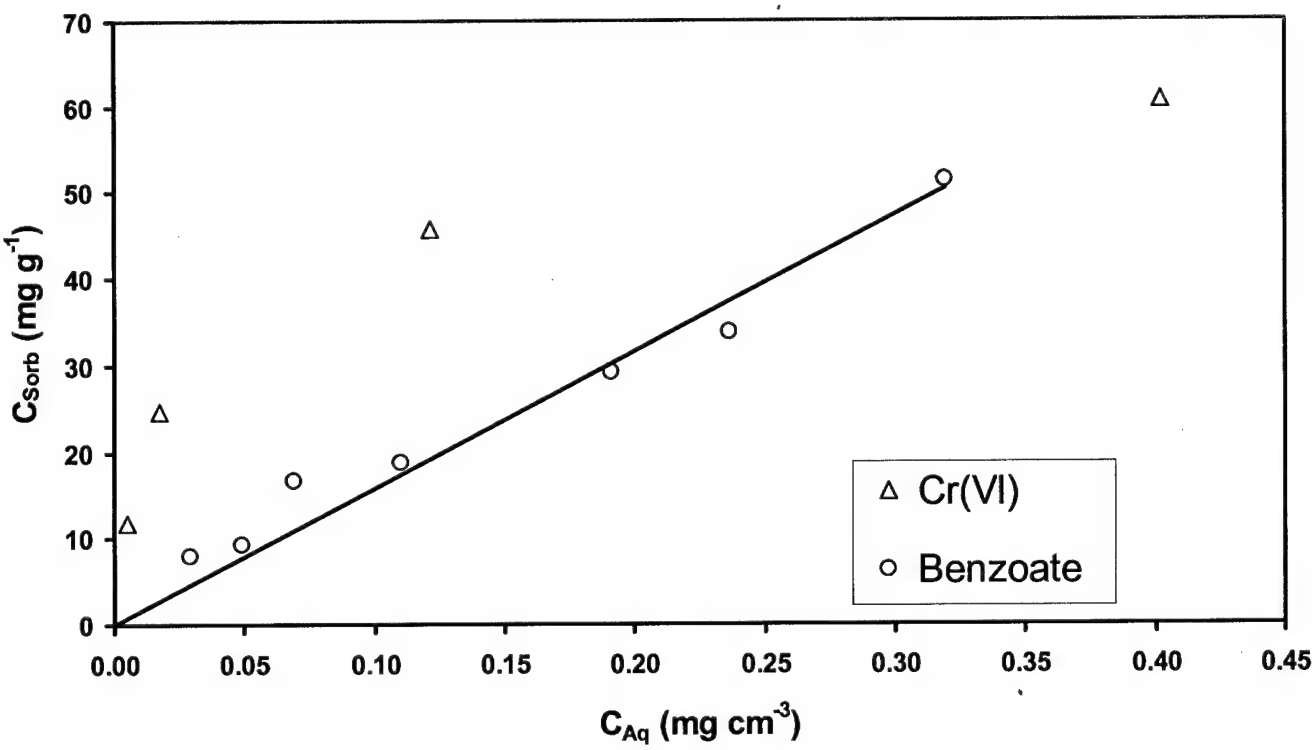

Figure 4. Cr(VI) and benzoate partitioning between SGB and AG1-X8(HCO_3^-) resin, pH 7, 20°C. Solid line corresponds to linear benzoate partitioning in SGB with $k_D^B = 158$ mL g^{-1}.

Parameters and masses of Cr(VI) and benzoate extracted from device sectors are summarized in Table 1 for the sixteen experimental runs. Experimental and measured

values of **q** and $\mathbf{J}^{Cr}$ were calculated as 2-dimensional vectors in a polar (r, θ) coordinate plane perpendicular to the device axis, with each vector having a radial (q_r, J_r^{Cr}) and an angular (q_θ, J_θ^{Cr}) component. The radial vector component is equivalent to vector magnitude, while the angular component is the vector direction. For each run in Table 1, time-averaged experimental (actual) values of $q_r\Delta t$ (m) and $J_r^{Cr}\Delta t$ (g m^{-2}) were calculated using

$$q_r \Delta t = \frac{\Delta V}{A^{Col}} \quad [3]$$

and

$$J_r^{Cr} \Delta t = \frac{\Delta V \cdot C_F^{Cr}}{A^{Col}} \quad [4]$$

Equations to calculate measured values of q_r and q_θ from extracted tracer masses m_i^B were derived from a simple center of mass analogy. The coordinates of the center of mass of a system of three point masses distributed in a rectangular (x, y) coordinate plane are given by $x_{cm} = \Sigma m_i x_i / \Sigma m_i$, $y_{cm} = \Sigma m_i y_i / \Sigma m_i$, where x_{cm} and y_{cm} are the coordinates of the center of mass, and x_i, y_i, and m_i are the coordinates and masses of the three point masses (*23*). These equations are converted to polar coordinates using $r_{cm} = (x_{cm}^2 + y_{cm}^2)^{0.5}$ and $\theta_{cm} = \tan^{-1}(y_{cm}/x_{cm})$. We can treat the mass of benzoate extracted from each sector of the device as a point mass located at the geometric center of the sector. In Figure 5, the x- and y-coordinates of the geometric centers of the three outer sectors are

Table 1. Parameters and extracted sector masses from 16 column experiments using permeable adsorbent devices.

Run No.	Experimental Parameters				Extracted Sector Masses (mg)					
					Cr(VI)			Benzoate		
	ΔV (L)	Δt (h)	q_θ (deg)	C_F^{Cr} (mg L^{-1})	m_1^{Cr}	m_2^{Cr}	m_3^{Cr}	m_1^{B}	m_2^{B}	m_3^{B}
1	4.80	49	0	4.8	0.14	0.44	0.16	0.20	0.13	0.20
2	10.3	25	0	5.7	0.30	1.09	0.36	0.15	0.05	0.13
3	20.4	76	0	4.8	0.51	1.60	0.42	0.15	0.01	0.19
4	30.2	75	0	4.9	0.83	2.48	0.96	0.17	0.02	0.13
5	5.30	45	45	4.8	0.03	0.39	0.23	0.20	0.12	0.20
6	11.7	74	45	5.0	0.06	0.81	0.65	0.35	0.16	0.18
7	20.8	115	45	4.8	0.26	1.35	1.98	0.41	0.11	0.04
8	41.9	158	45	5.2	0.49	3.16	3.33	0.50	0.05	0.02
9	5.00	20	90	4.8	0.07	0.24	0.38	0.18	0.09	0.12
10	8.30	98	90	5.0	0.20	0.51	0.73	0.31	0.24	0.15
11	20.0	95	90	4.8	0.40	0.99	1.76	0.29	0.13	0.03
12	40.9	167	90	5.2	0.67	1.67	2.51	0.31	0.09	0.02
13	4.60	45	180	4.8	0.31	0.32	0.39	0.19	0.11	0.08
14	9.80	77	180	5.0	0.75	0.70	0.78	0.12	0.25	0.13
15	19.2	114	180	4.8	1.23	0.80	1.53	0.07	0.30	0.07
16	39.7	146	180	5.2	1.98	1.80	3.50	0.08	0.22	0.02

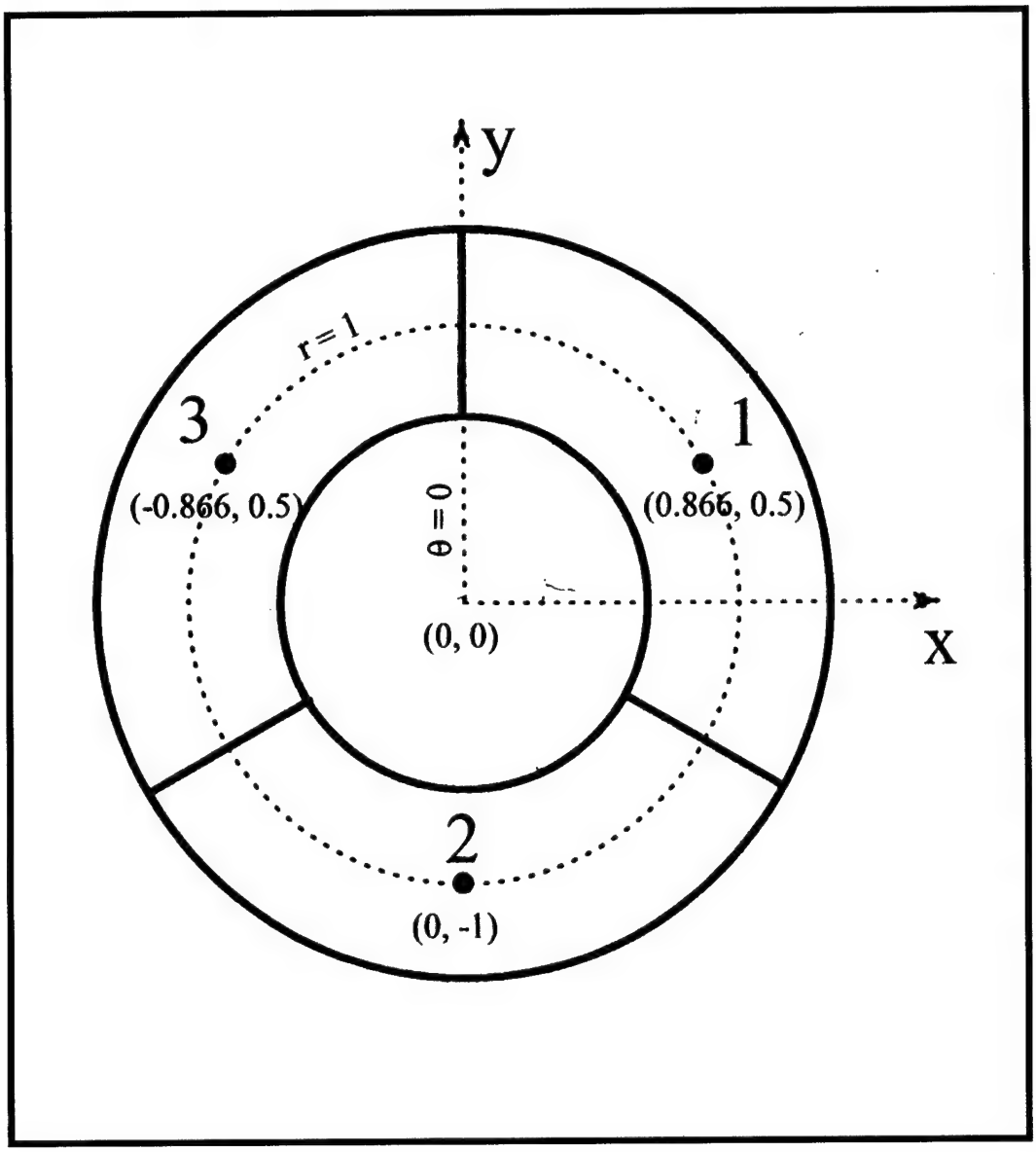

Figure 5. Axial view of device, showing rectangular (x, y) coordinates of the geometric centers of the three outer sectors, and polar reference lines $r = 1$ and $\theta = 0$.

indicated, along with the rectangular axes of the system. The circle r = 1 is located midway between the center well perimeter and the device outer wall, and the line θ = 0 is set parallel to the divider between sectors 1 and 3. Using this reference system along with the equations for r_{cm} and θ_{cm} above, we can now calculate the polar coordinates of the center of mass of the benzoate within the device (r_{cm}^{B}, θ_{cm}^{B}) as

$$r_{cm}^{B} = \frac{D^{Dev} + D^{CW}}{4} \sqrt{\left[\frac{0.866\left(m_1^B - m_3^B\right)}{m_1^B + m_2^B + m_3^B}\right]^2 + \left[\frac{0.5\left(m_1^B + m_3^B\right) - m_2^B}{m_1^B + m_2^B + m_3^B}\right]^2} \qquad [5]$$

$$\theta_{cm}^{B} = \tan^{-1}\left[\frac{0.866\left(m_1^B - m_3^B\right)}{0.5\left(m_1^B + m_3^B\right) - m_2^B}\right] \qquad [6]$$

Note that [5] and [6] do not include the mass of benzoate in the center well. By locating the origin of the coordinate system at the device axis, the coordinates of the geometric center of the center well are (0, 0), so any benzoate mass in the center well makes no contribution to the center of mass calculation. The term $(D^{Dev} + D^{CW})/4$ in [5] is the distance (cm) from the device axis to midway between the center well perimeter and the outer wall, while the radical term calculates the fraction of this distance that the center of mass of the resident tracer zone has been displaced. Equation [6] applies as shown when $(m_1^B + m_3^B)/2 \geq m_2^B$; otherwise the negative of [6] is used. A relationship between r_{cm}^{B} and q_r can be derived from solute transport theory. Since benzoate equilibrium partitioning is linear, we can neglect skewing of the resident tracer zone due to nonlinear

effects. Then, neglecting effects of dispersive transport, the rate v_r^B of benzoate advective transport within the device is related to q_r by

$$v_r^B = \frac{q_r}{R^B} \quad [7]$$

At the same time, v_r^B can be measured from r_{cm}^B using

$$v_r^B = \frac{r_{cm}^B}{\Delta t} \quad [8]$$

Equating [7] and [8], substituting in [5], solving for the time-averaged quantity $q_r\Delta t$, and then inserting K^{Corr} to correct for hydraulic conductivity differences gives

$$q_r \Delta t = \frac{R^B K^{Corr}\left(D^{Dev} + D^{CW}\right)}{4}\sqrt{\left[\frac{0.866\left(m_1^B - m_3^B\right)}{m_1^B + m_2^B + m_3^B}\right]^2 + \left[\frac{0.5\left(m_1^B + m_3^B\right) - m_2^B}{m_1^B + m_2^B + m_3^B}\right]^2} \quad [9]$$

Measured values of Cr(VI) mass flux $J_r^{Cr}\Delta t$ were simply calculated from extracted Cr(VI) masses using

$$J_r^{Cr}\Delta t = \frac{K^{Corr}\left(m_1^{Cr} + m_2^{Cr} + m_3^{Cr}\right)}{L^{Dev}D^{Dev}} \quad [10]$$

The product $L^{Dev}D^{Dev}$ in the denominator of [10] represents the projected area of the device normal to incident flow.

Figure 6 shows q_θ results calculated using [6] from the sixteen sets of m_i^B data in Table 1. Measured q_θ values are plotted against experimental parameters. For experiments with $\Delta V \geq 8.3$ L ($q_r\Delta t \geq 0.83$ m) average residual error of measured q_θ

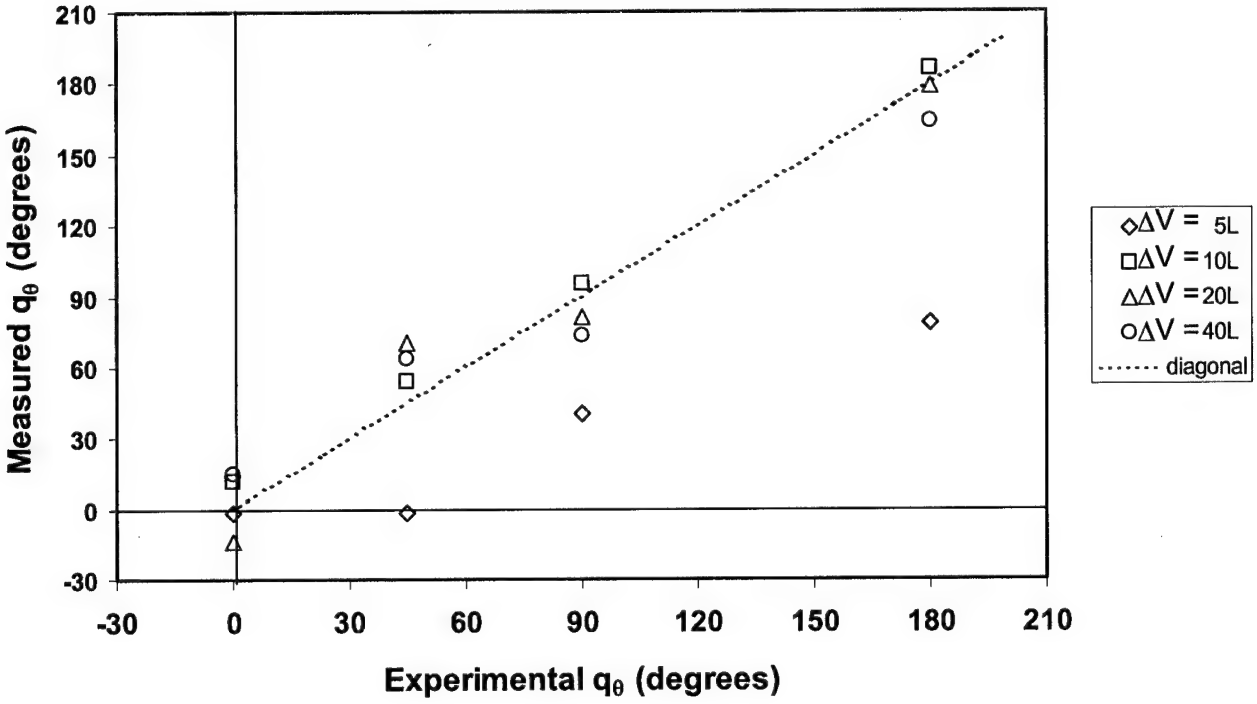

Figure 6. Angular component of specific discharge vector (q_θ), measured values from [6] versus experimental values for the 16 runs. Dashed line is diagonal for reference.

values was 12 degrees, while the four experiments with $\Delta V \leq 5.3$ L had average residual q_θ error of 50 degrees. These results demonstrate that a minimum fraction of resident tracer must be displaced out of the device center well for accurate measurement of q_θ.

Measured $q_r \Delta t$ values calculated using [9] are plotted in Figure 7(a) against experimental values calculated from [3]. Fair accuracy was obtained for experiments

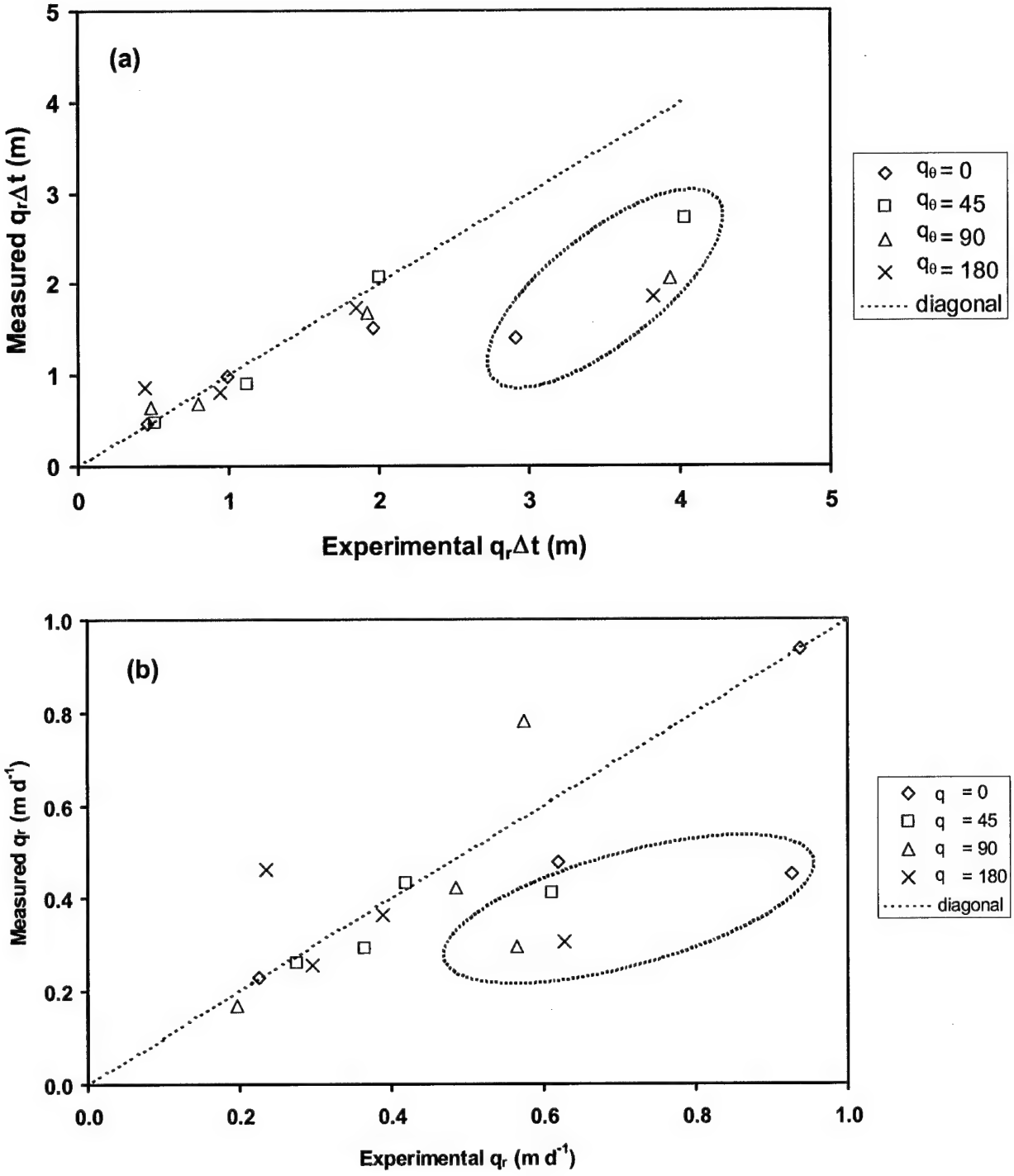

Figure 7. Radial component of specific discharge vector. (a) Time-averaged specific discharge ($q_r\Delta t$, m), measured values from [9] versus experimental values from[3]. (b) Specific discharge (q_r), measured versus experimental values.

with $\Delta V < 20$ L ($q_r\Delta t < 2.0$ m), with relative residual error for those runs averaging 19%. Poorest accuracy was observed for the four experiments with $\Delta V > 28$ L ($q_r\Delta t > 2.8$ m; runs 4, 8, 12, and 16 in Table 1, and circled points in Figure 7), for which relative residual error averaged 46%. This loss of accuracy with increasing $q_r\Delta t$ can be explained by using [7] and [8] to calculate that for $q_r\Delta t > 3.0$ m, $r_{cm} > 1.3$ cm. This means that for those four experiments a significant amount of benzoate resident tracer had begun to elute off of the downstream edge of the device. Resident tracer can be transported within the device by both dispersive and advective processes. Dispersive processes should have the effect of broadening the resident tracer zone without displacing its center of mass. Note in Table 1 that benzoate was detected in all three outer sectors in every experiment, including those sectors that were upgradient of the center well. This observation can only be explained by dispersion, or broadening of the resident tracer zone during the experiments. Dispersive transport of resident tracer can contribute to non-quantitative loss of tracer off of the device. Non-quantitative loss of resident tracer from the device would increase by advection as $q_r\Delta t$ increases and by dispersion as Δt increases. This non-quantitative tracer loss causes the apparent migration of the tracer zone center of mass to stall. This explains the observation in Figure 7(a) that measured $q_r\Delta t$ values did not increase past 3.0 m. Figure 7(b) is a plot of the q_r values obtained by applying the trivial calculation $q_r = q_r\Delta t/\Delta t$ to the $q_r\Delta t$ values obtained from [9] and [3]. Excluding the four circled points, the average residual error in measured q_r values was 19%.

Figure 8(a) shows measured $J_r^{Cr}\Delta t$ values calculated from the extracted Cr(VI) masses in Table 1 using [10] plotted against experimental $J_r^{Cr}\Delta t$ values calculated using [4]. Good agreement between measured and experimental values was observed over the sixteen runs. Although Cr(VI) was detected in each outer sector extract from every run, no Cr(VI) was detected in center well extract for any of the runs (data not shown). This observation shows that Cr(VI) was not breaking through the adsorbent in the upgradient sectors. The good quantitative Cr(VI) recovery shown in Figure 8 combined with observed lack of breakthrough into the center well demonstrates that any Cr(VI) transported into the device was effectively bound by the adsorbent. Absence of Cr(VI) in center well extracts also shows that competition for adsorption sites between Cr(VI) and benzoate was not a significant factor in observed benzoate migration rates. The masses of Cr(VI) extracted from downgradient sectors as shown in Table 1 are evidence of dispersive transport through the outer shell of the device. Figure 8(b) shows the accuracy of values obtained using $J_r^{Cr} = J_r^{Cr}\Delta t/\Delta t$ with the $J_r^{Cr}\Delta t$ results from [4] and [10] for the sixteen column experiments. Average residual error in measured J_r^{Cr} values was 17%. Using an equation analogous to [6] to calculate J_θ^{Cr} from extracted Cr(VI) masses gave poor agreement with experimental q_θ values (results not shown). This is because Cr(VI) accumulates over the entire outer edge of the adsorbent bed, so that a small amount of quantitative error introduced during adsorbent removal, extraction, and analysis translates to large error in J_θ^{Cr} values calculated using [6]. However, it is reasonable to assume that $J_\theta^{Cr} = q_\theta$ for any flow situation in which advective Cr(VI) transport dominates over other

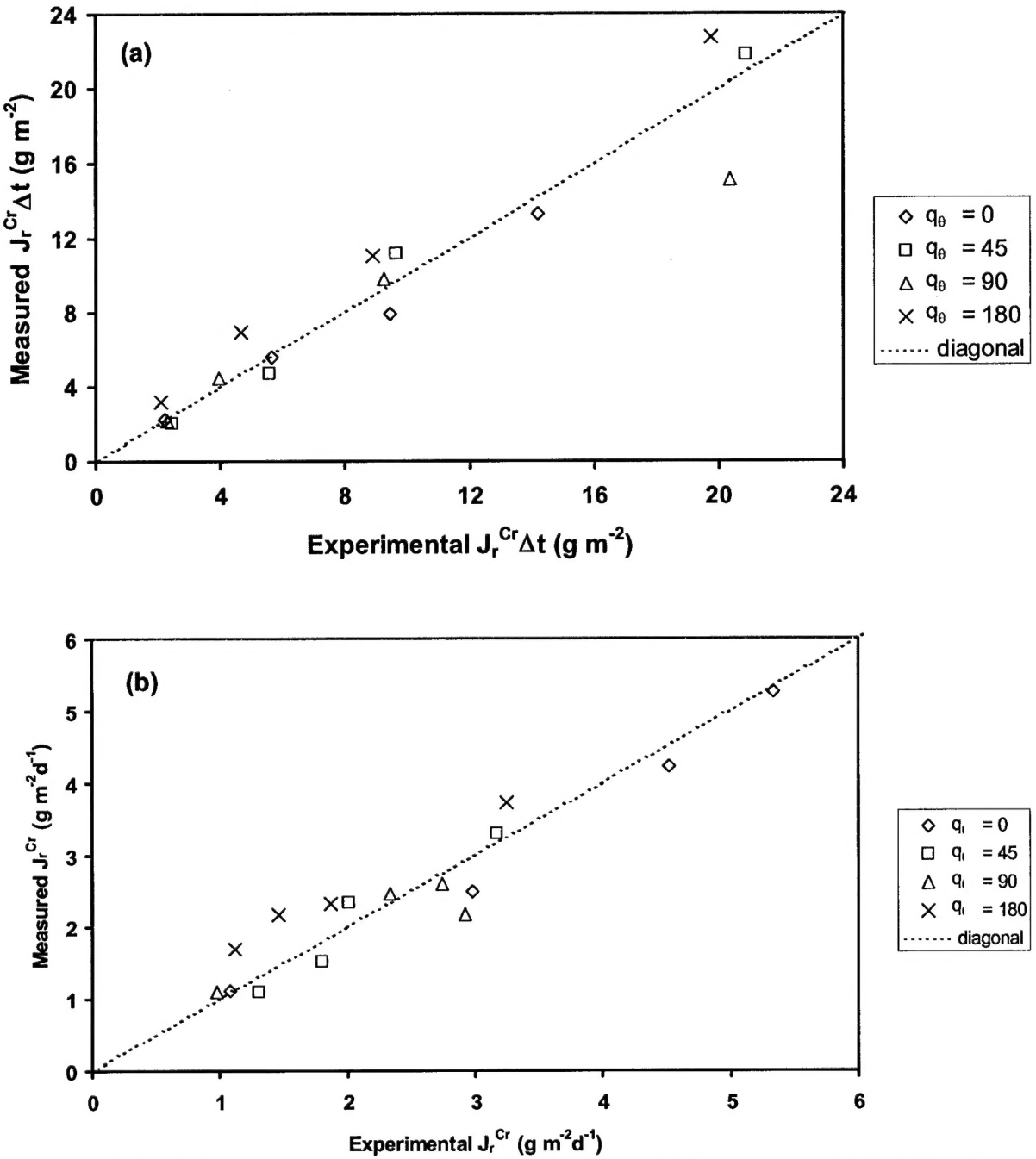

Figure 8. Radial component of Cr(VI) mass flux vector. (a) Time-averaged Cr(VI) mass flux ($J_r^{Cr}\Delta t$), measured values from [10] versus experimental values from [4]. (b) Cr(VI) mass flux (J_r^{Cr}), measured versus experimental values.

processes. An example where this would not be the case is when the device is located in a slow flow field within a Cr(VI) concentration gradient, which could allow dispersive transport to dominate over advection, so that $J_\theta^{Cr} \neq q_\theta$. Even in such an unusual situation, however, sampling over long Δt would allow time for the gradient to dissipate, so that over the course of the sampling period q_θ would approach J_θ^{Cr}.

Modification of the device design and of the procedures described in this paper could possibly improve the accuracy of the technique. The devices used in these experiments had center wells one-half the device outer diameter. This design gives four sectors of equal volume. However, using a larger D^{Dev}/D^{CW} ratio could increase the range over which accurate q_r values are obtained, as this would allow the resident tracer to migrate farther before eluting off the downstream edge of the device. Using finer-grained adsorbent and resident tracers with higher k_D values would minimize the effects of dispersive transport processes, possibly increasing the accuracies of measured q_θ, q_r, and J_r^{Cr} values. It should be possible to load a set of resident tracer compounds with various k_D values onto the center well adsorbent, allowing accurate measurement of q_r over a broader range of $q_r\Delta t$ values. An example of another anionic compound appropriate for use as resident tracer is pentafluorobenzoate, which was found to partition linearly in SGB/AG1-X8(HCO_3^-) system, with k_D = 401 mL/g (data not shown). Sampling over long periods in groundwater with high q_r and ionic strength would require

the use of a resident tracer with high k_D, while short sampling periods, low q_r and low groundwater ionic strength would require the use of highly mobile resident tracers.

The results of the laboratory experiments reported above demonstrate the potential utility of permeable adsorbent devices for simultaneous measurement of local groundwater specific discharge and Cr(VI) mass flux in contaminated aquifers, and more generally for monitoring transport and attenuation rates of various groundwater contaminants. Further study is needed to test the accuracy and practicality of these devices in actual field conditions.

Acknowledgments

This research was partially funded the by the U.S. Department of Defense (project number 200114) under the Environmental Security Technology Compliance Program (ESTCP), and by the U.S. Department of Energy (DE-FG02-97ER62471) under Natural and Accelerated Bioremediation Research (NABIR) program. The authors gratefully acknowledge the support of Thomas B. Stauffer of the U.S. Air Force Research Laboratory (AFRL/MLQ) for providing laboratory facilities at Tyndall Air Force Base, Florida, where the experiments were conducted.

Literature Cited

1. National Research Council. *Environmental Epidemiology, Vol. 1, Public Health and Hazardous Wastes*; National Academy Press: Washington, DC, 1991; p.108.
2. Deng, B.; and Stone, A.T. *Environ. Sci. Technol.* **1996**, *30*, 2484-94.
3. Kozuh, N.; Stupar, J.; and Gorenc, B. *Environ. Sci. Technol.* **2000**, *34*, 112-119.
4. Chen, J. M.; and Hao, O.J. *Crit. Rev. Environ. Sci. Technol.* **1998**, *28*, 219-251.
5. Lovley, D.R. *J. Ind. Microbiol.* **1995**, *14*, 85-93.
6. Shen, H.; Pritchard P.H.; and Sewell, G.W. *Environ. Sci. Technol.* **1996**, *30*, 1667-1674.
7. Mikami, N.; Sasaki, M.; Kikuchi, T.; Yasunaga, T. *J. Phys. Chem.* **1983**, *87*, 5245-5248.
8. Ainsworth, C.C.; Girvin, D.C.; Zachara, J.M.; Smith, S.C. *Soil Sci. Soc. Am. J.* **1989**, *53*, 411-418.
9. Zachara, J.M.; Girvin, D.C.; Schmidt, R.L.; Resch, C.T. *Environ. Sci. Technol.* **1987**, *21*, 589-594.
10. Sag, Y.; Atacoglu, I.; and Kutsal, T. *Sep. Sci. Technol.* **1999**, *34*, 3155-71.
11. Schroeder, D.C.; Lee, G.F. *Water Air Soil Pollut.* **1975**, *4*, 355.
12. Hug, S.H.; Laubscher, H.U.; James, B.R. *Environ. Sci. Technol.* **1997**, *31*, 160-170.
13. Baes, C.F.; Mesmer, R.E. The hydrolysis of cations. Wiley-Interscience, New York, 1976.